DINAME 2017 - Proceedings of the XVII International Symposium on Dynamic Problems of Mechanics
A. T. Fleury, D. A. Rade, P. R. G. Kurka (Editors), ABCM, São Sebastião, SP, Brazil, March 5-10, 2017

DINAME 2017 – Optimization of Equivalent Damping Coefficient of Thrust Bearings

Thales Freitas Peixoto[1], **Gregory Bregion Daniel**[2], **Katia Lucchesi Cavalca**[3]

[1, 2, 3] Laboratory of Rotating Machinery, Faculty of Mechanical Engineering, University of Campinas, 200 Mendeleyev Street, 13083-860, Campinas, São Paulo, Brazil
[1] thalesfp@fem.unicamp.br
[2] gbdaniel@fem.unicamp.br
[3] katia@fem.unicamp.br

Abstract: A specific class of rotary machines is the high rotation turbochargers, to automotive application, wherein the shaft is continually subjected to axial forces of different magnitudes due to gas flows in the turbine and the compressor. These forces are supported by axial lubricated thrust bearings. The thrust bearings are modeled through equivalent stiffness and damping coefficients and the objective of the work is to get good estimates of these coefficients, comparing simulated results with experimental results. The stiffness coefficient is first obtained by small perturbation around the equilibrium position and used in a finite element model of the system at specific rotational speeds, and this value is compared to experimental results. Then, the damping coefficient is estimated, by running an optimization problem on this parameter, to approximate the simulated dynamic response of the system to experimental results of the turbocharger excited by an impact hammer, where both the displacement and force were measured.

Keywords: Hydrodynamic thrust bearing, Stiffness Coefficient, Damping Coefficient

NOMENCLATURE

Latin symbols

$\mathbf{A}$: state space matrix
$\mathbf{b}(t)$: excitation vector
C_{xx}**:** equivalent viscous damping coefficient
$F(t)$: excitation force
h: oil thickness
K_{xx}: equivalent stiffness coefficient
M: total mass of the system
min: minimum operator
max: maximum value of array
r: radius of thrust bearing
t: time
v: velocity
$x(t)$: displacement
$\dot{x}(t)$: velocity
$\ddot{x}(t)$: acceleration
$\mathbf{y}(t)$: state space vector

Greek symbols

θ: angular length of the bearing pad
ξ : viscous damping factor
ω_n: natural frequency

Subscripts

0: relative to initial conditions/total arc length of pad
1: relative to thrust bearing 1
2: relative to thrust bearing 2
exp: relative to experimental results
i: relative to the inner radius
max: relative to the upper bound on the design variable/maximum oil thickness
min: relative to the lower bound on the design variable
o: relative to the outer radius
ramp: relative to arc length of the pad ramp
sim: relative to the simulated results
xx: relative to axial (longitudinal) direction

INTRODUCTION

A shaft is a rotating member of circular cross section used to transmit power and motion. A rotary machine is the assembly of a rotating shaft supported by bearings, with one or more rotors (turbine or compressor, for example). A very specific class of rotary machines is the high rotation turbocharges, to automotive application. The turbocharger is an equipment added to internal combustion engines to raise its power or efficiency, using the exhausting gases of the engine to move the turbine attached to a compressor. The compressor raises the air pressure entering the combustion chamber of the engine, allowing a larger mass flow rate than is possible in a naturally aspirated engine (Korpela, 2011).

The turbochargers have, essentially, four elements: the rotating shaft, the turbine, the compressor, and the bearings. The radial inflow turbine is the element that drives the whole system. The centrifugal compressor is the element that improves the combustion process and the shaft is responsible for transferring the energy produced by the turbine to the compressor.

The bearings are responsible for supporting the loadings in the shaft. Because of unbalanced mass, inherently to every rotating system, there is radial vibration in the shaft, which must be supported by journal bearings. Moreover, the gas flows in the turbine and the compressor are not constant and these flows produce radial and axial forces of different amplitudes. The axial forces produce axial displacements that are not supported by the journal bearings. To support this axial displacement, the use of thrust bearings is necessary, to absorb the axial loadings and displacements of the shaft. The thrust bearings must be designed to let the oil film between the bearing and the collar attached to the shaft sustain the shaft axially, avoiding contact between the surfaces in relative motion, to mitigate friction and premature wear of these surfaces (Vieira, 2014).

The axial vibration of the entire turbocharger is the object of analysis. It is assumed that this vibration can be modeled by concentrated parameters (a one degree of freedom system, represented by a linear second order differential equation) and the thrust bearings can be approximated by its dynamic characteristics, i.e., its equivalent damping and stiffness coefficients. Lund (1987) introduced the concept to approach the dynamic characteristics of bearings through its equivalent coefficients, which basically consists in solve the governing equation for the pressure distribution to find the equilibrium position of the system and recalculate its equation applying small perturbations around the previously found equilibrium position.

The governing equation for the pressure distribution in lubricated bearings is the Reynolds' Equation (Reynolds, 1886), a second order partial differential equation governing the pressure distribution of thin viscous fluid films, which can be derived from the Navier-Stokes equations neglecting the terms of higher orders that consider the (small) thickness of the oil film. Specifically to thrust bearings, Hamrock, Schmid and Jacobson (1994) obtained an analytical solution to bearings whose radial dimensions of the pads were much higher than its circumferential dimensions. With this assumption, the radial flows crossing the interface between the bearing and the collar (shaft) can be neglected. This solution, however, is not always adequate, since the oil flow in the radial direction can be considerable, depending on the radial and circumferential dimensions of the thrust bearings. Pinkus was the first to obtain a numerical solution to the Reynolds' Equation. Pinkus and Lynn (1958) obtained a solution by the Finite Difference Method to thrust bearings, whose oil film thickness linearly varies with the circumferential length.

Pinkus idea to apply numerical methods to solve the Reynolds' Equation was not restricted to hydrodynamic analysis (HD analysis), considering other effects in the bearings, besides the pressure distribution and the hydrodynamic forces. Numerical methods began to consider thermal effects on the bearings creating the thermo-hydrodynamic analysis (THD analysis). Dowson (1962) published one of the main works in the THD analysis, deriving the generalized Reynolds' Equation, which takes into account the variation of fluid properties, such as the viscosity and density and his work contributed to future works that covered the THD lubrication. Recent works in solving the Reynolds' Equation in thrust bearings can be cited, such as Arghir, Alsayed and Nicolas (2002), that utilized the Finite Volume Method to obtain the pressure distribution in thrust bearings with discontinuities in the oil film and Alqmvist, Glavatskih and Larsson (2000), that compared simulated THD results with experimental results. Dadouche, Fillon e Bligoud (2000) empirically observed the influence of various parameters, such as axial load applied, rotation speed and the replacement oil temperature, over the pressure and temperature field in the bearings. Dadouche, Fillon and Dmochowski (2006) compared experimental results obtained in the previous experimental bench with simulated results. Finally, Ahmed, Fillon and Maspeyrot (2010) based their work in Dowson equation to obtain a solution to the THD problem using the generalized Reynolds' Equation to thrust bearings.

In this paper, the coefficients are estimated using experimental results. Daniel, Vieira and Cavalca (2016) estimated the stiffness coefficient, first solving the governing equations for the journal bearings to estimate the inlet temperature of the oil in the thrust bearing, necessary to solve the generalized Reynolds' Equation of thrust bearings taking into account thermal effects. The objective of this paper is to estimate the equivalent damping coefficient of the system, by running an optimization algorithm so that a simulated transient response of the shaft displacement matches the measured displacement of the shaft.

MATERIALS AND METHODS

A scheme of the turbocharger is shown in Fig. 1. The turbocharger in Fig. 1a consists of a turbine and a compressor attached to the shaft, supported by two thrust bearings. This turbocharger can be modeled by the equivalent system in Fig. 1b, considering that there is only relative motion between the collar and the thrust bearings, increasing or decreasing the oil film thickness. It is assumed that the thrust bearings are clamped and the collar moves only in the axial direction (defined as the x coordinate). The thrust bearings support the external forces ΔF to maintain the system working properly. The springs and viscous dampers are the equivalent coefficients of the oil film between the bearings and the collar. The collar bearing has an outer diameter of 30 mm, a thickness of 1,5 mm and a clearance of 49.9 μm (equal for both bearings). The geometric dimensions of the thrust bearings are shown in Tab. 1, through the ratios of the main design parameters. The main variables of the thrust bearings, also shown schematically in Fig. 2, are the inner (r_i) and outer (r_o) radius, the angular length of the pad ramp (θ_{ramp}), the angular length of the pad (θ_0), the minimum (h_0) and maximum ($h_{\max}$) oil thickness and the number of pads (n_{pad}) of the bearing.

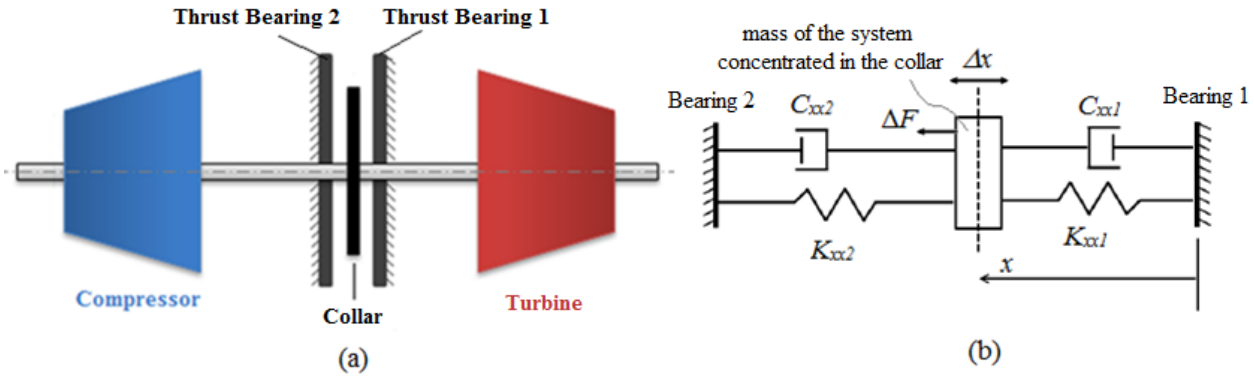

Figure 1 – (a) Scheme of turbocharger and (b) Equivalent system of springs and viscous dampers of the thrust bearing

Table 1 – Geometric ratios of the bearings (Vieira, 2014)

Variable	Bearing 1	Bearing 2
r_o / r_i	1,5	1,7
r_i / h_0	350	340
$h_{\max} / h_0$	2,4	2,0
$\theta_{ramp} / (\theta_0 - \theta_{ramp})$	5,0	4,0
n_{pad}	3	3

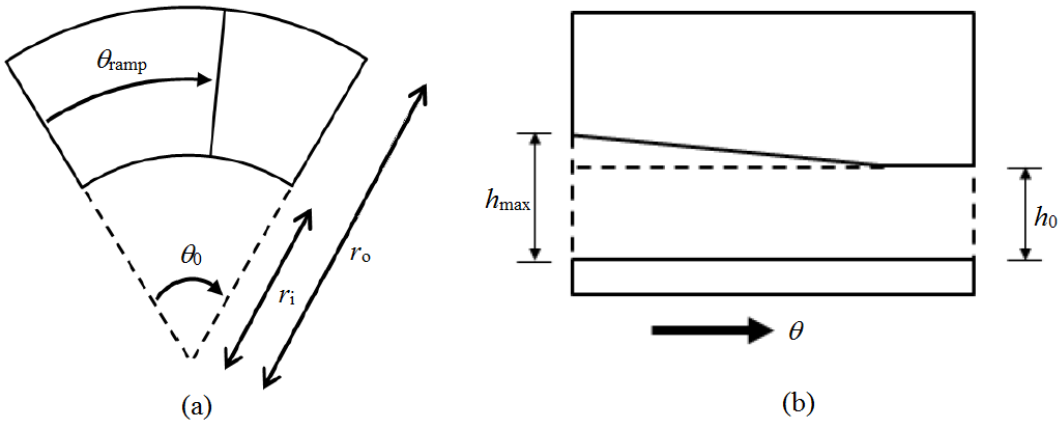

Figure 2 – (a) Bearing pad and (b) Fluid thickness profile (Adapted from Vieira, 2014)

The axial vibration of the turbocharger is modeled here as a one degree of freedom system (Vieira, 2014). The governing dynamic equation is obtained admitting that the entire mass *M* of the system is concentrated in the collar of the shaft and the springs and dampers of Fig. 1b are in parallel to each other. Since the springs and dampers are in parallel, the equivalent stiffness and damping coefficients are the sum of the coefficients of Fig. 1b, $K_{xx} = K_{xx1} + K_{xx2}$ and $C_{xx} = C_{xx1} + C_{xx2}$. Therefore, the equation of motion of the system shown in Fig. 1b is:

$$M\ddot{x}(t) + C_{xx}\dot{x}(t) + K_{xx}x(t) = F(t) \tag{1}$$

which can be evaluated numerically, by integrating Eq. (1) using the state space model defined as (Müller and Schiehlen, 1985):

$$\dot{\mathbf{y}}(t) = \mathbf{A}\mathbf{y}(t) + \mathbf{b}(t) \tag{2}$$

where the state space vector $\mathbf{y}(t)$ is defined as $[x(t) \quad \dot{x}(t)]^t$, $\mathbf{A}$ is the state space matrix and $\mathbf{b}(t)$ is the excitation vector, both defined as

$$\mathbf{A}=\begin{bmatrix} 0 & 1 \\ -\dfrac{K_{xx}}{M} & -\dfrac{C_{xx}}{M} \end{bmatrix}, \quad \mathbf{b}(t)=\begin{Bmatrix} 0 \\ \dfrac{F(t)}{M} \end{Bmatrix} \tag{3}$$

In the test condition, the turbine is driven by compressed air, while the compressor is open to the atmosphere. The system is axially excited by an impact hammer, in the shaft end. The axial displacement of the system is measured, utilizing a displacement sensor, as well as the force applied by the hammer, in time domain, as illustrated in Fig. 3.

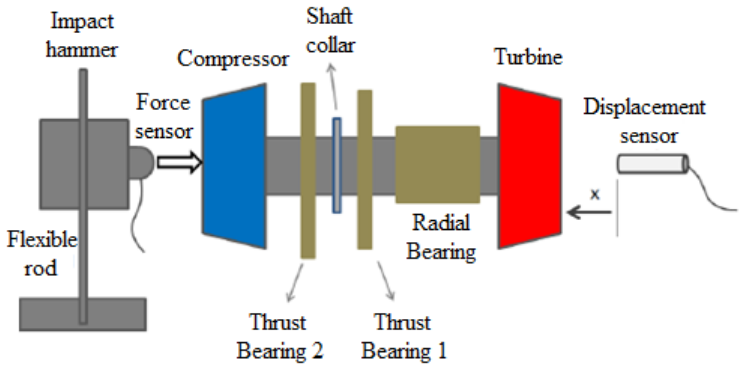

Figure 3 – Scheme of experimental setup of the turbocharger (Adapted from Vieira, 2014)

The aim of this work is to estimate the equivalent coefficients of the bearings, so the simulated response of the system is compatible with the experimental results obtained, due to an impulsive excitation force. The stiffness coefficient of the system can be estimated as described by Daniel, Vieira and Cavalca (2016), which consists in solving the Reynolds' Equation utilizing a thermo-hydrodynamic (THD) model, by the Finite Volume Method, to obtain the pressure distribution of the oil film circulating in the thrust bearings, accounting for parameters like the geometry of the bearings and the temperature distribution in the oil film.

The Reynolds' Equation is the governing equation for pressure distribution in the oil film. To account for the variation of temperature of the oil film, which changes the oil viscosity along the bearing, the generalized Reynolds' Equation must be utilized. This equation was introduced by Dowson (1962) and is written in cylindrical coordinates as

$$\frac{1}{r}\frac{\partial}{\partial\theta}\left(F_2\frac{\partial p}{\partial\theta}\right)+\frac{\partial}{\partial r}\left(rF_2\frac{\partial p}{\partial r}\right)=\Omega r\frac{\partial}{\partial\theta}\left(\frac{F_1}{F_0}\right)+r\frac{\partial h}{\partial t} \tag{4}$$

in which Ω is the rotational speed of the shaft and the functions F_0, F_1 and F_2 are introduced to account for the temperature distribution in the oil film, which changes the oil viscosity (μ) along the mesh. These functions are defined as

$$F_0=\int_0^h\frac{1}{\mu}dx, \quad F_1=\int_0^h\frac{x}{\mu}dx, \quad F_0=\int_0^h\frac{x}{\mu}\left(x-\frac{F_1}{F_0}\right)dx \tag{5}$$

These integrals are responsible for the coupling between the viscosity variation along the oil film and the pressure to be calculated by the generalized Reynolds' Equation (Eq. 4).

Daniel, Vieira and Cavalca (2016) approached the problem to obtain the equivalent stiffness coefficient of the thrust bearing as suggested by Lund (1987), by solving the generalized Reynolds' Equation after applying little perturbations around the equilibrium position previously calculated, disregarding the fluid film variation with the time $(\partial h/\partial t=0)$. However, to estimate this coefficient, it is necessary to observe that the circulating oil in the thrust bearing enters the turbocharger through journal bearings, which causes an increase in its temperature. A THD model of the journal bearing is first solved to estimate the temperature of the oil leaving the journal bearing, assumed as the temperature of the oil inlet in the thrust bearing.

The results obtained by Daniel, Vieira and Cavalca (2016) can be checked using the one degree of freedom equation (Eq. 1) and a finite element method to discretize the turbocharger, following the method suggested by Peixoto, Vieira and Cavalca (2015) and Peixoto (2016). Peixoto, Vieira and Cavalca (2015) compared the natural frequency of the system obtained by the one degree of freedom system, by a finite element solution and the equation of longitudinal vibration of uniform bars with discontinuities of concentrated masses and springs. Peixoto (2016) calculated the oil thickness of the fluid in the thrust bearing, using a step force and the equivalent stiffness coefficient calculated in the simulations of Daniel, Vieira and Cavalca (2016), comparing the values with measured, empirical results.

The oil thickness was calculated according to Fig. 4. The oil thickness of each thrust bearing is originally h_{01} and

h_{02}, for the thrust bearings 1 and 2, respectively. The collar attached to the shaft changes its equilibrium position by an amount Δx after an external excitation, modeled as a step excitation, acts on the system. The collar changes its static equilibrium position due to the step excitation, which causes the oil thickness to change an amount equal to

$$h_0\big|_{new} = h_0 \pm \Delta x \tag{6}$$

The minimum estimated oil thickness of the bearing is $h_0 - |\Delta x|$ and this value is compared to the experimental measurements.

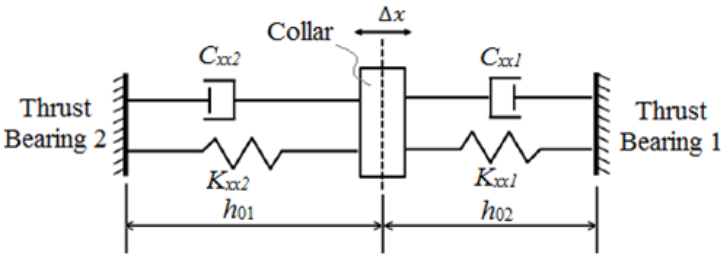

Figure 4 – Simplified scheme of the assembly bearings and collar (Adapted from Peixoto, 2016)

To check the change of oil thickness in the model means to check if the estimated stiffness coefficient is the same as obtained in the experimental results. The stiffness coefficient alone, however, changes only the static equilibrium position of the system, but gives little information on the dynamic response of the system. It is also necessary to obtain the equivalent damping coefficient to fully add the flexibility of the oil film in the dynamic response of the system. The damping coefficient is estimated by optimizing this parameter, setting as the objective function the maximum absolute difference between the simulated response and the experimental response. The optimization algorithm utilized is the interior point algorithm (Byrd *et al*, 1999, and Byrd *et al*, 2000).

The optimization problem is constructed admitting that the objective function to minimize is the maximum absolute difference between the experimental response ($\mathbf{x}_{\exp}$) and the simulated response ($\mathbf{x}_{sim}$):

$$\min_{c_{\min} \le c \le c_{\max}} \left(\max \left(\left| \mathbf{x}_{sim} - \mathbf{x}_{\exp} \right| \right) \right) \tag{7}$$

The vector $\mathbf{x}_{\exp}$ is obtained from experimental measured results (Vieira, 2014), along with the time vector $\mathbf{t}$, while the simulated response $\mathbf{x}_{sim}$ is obtained from the numerical integration of the system given by Eq. 2.The input force for the simulation of the system is the input force measured in the impact hammer, during the experiment. It is important to notice that the *max* function in Eq. 7 returns the highest value of the array $\left| \mathbf{x}_{sim} - \mathbf{x}_{\exp} \right|$, where $|\mathbf{v}|$ is the element-wise absolute value function of the vector $\mathbf{v}$, while $\min(f(x))$ is the *min* operator, which returns the minimum value of the function $f(x)$.

The system is numerically integrated, with initial conditions $x_0 = 0$, i.e., the system starts from rest, and $\dot{x}_0 = v_0$, i.e., with an initial velocity given by:

$$v_0 = \frac{dx}{dt} \cong \frac{x[2] - x[1]}{t[2] - t[1]} \tag{8}$$

so, the initial velocity of the system is estimated by the forward difference approximation, utilizing the measured values of displacement and time. The optimization problem is solved using the `fmincon` function from MATLAB®, to find constrained minimum of a function, using the interior point algorithm (Byrd *et al*, 1999, and Byrd *et al*, 2000). The constrain is the range admitted for the damping coefficient, in the case studied here, $0 < c < 10^6$ N.s/m.

RESULTS

The turbocharger analyzed here has a total mass of 165 g. For a rotational speed of 14,100 rpm, the results obtained in the experiment schemed in Fig. 3 are shown in Fig. 5. Figure 5a shows the applied force by the impact hammer as a function of time and Fig. 5b shows the axial displacement measured as a function of time.

The clearance of the thrust bearing is 49.9 μm and, for this operation condition, the measured minimum oil thickness is 23.8 μm. For this test condition, the replacement oil temperature entering the turbocharger was measured in 37 °C and the temperature of the inlet oil in the thrust bearing was estimated in 60.6 °C, by Daniel, Vieira and Cavalca (2016).

Then, the equivalent stiffness coefficient and the force supported by each thrust bearing in Fig. 2 were estimated and shown in Tab. 1.

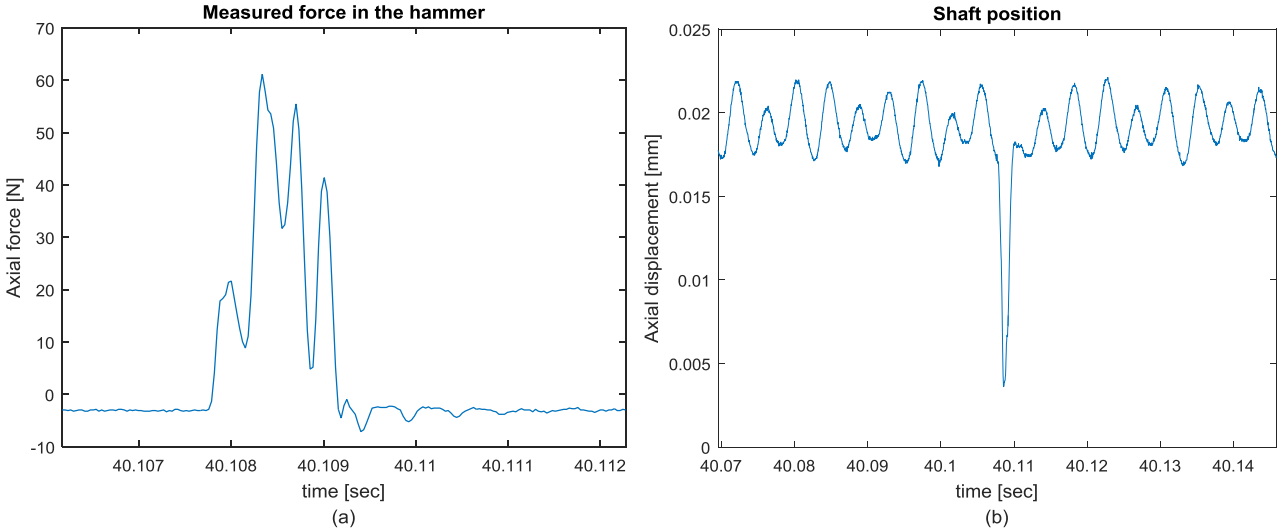

Figure 5 – Experimental results: (a) Force measured in the impact hammer and (b) Axial displacement of the shaft

Table 2 – Estimated supported forces and equivalent stiffness coefficients of the thrust bearings, for a rotation speed of 14,100 rpm (Adapted from Daniel, Vieira and Cavalca, 2016)

Thrust Bearing	Supported Force (N)	Equivalent Stiffness Coefficient (10^6 N/m)
1	32.75	2.264
2	-38.03	4.460

The equivalent stiffness coefficient is, therefore, 6.724×10^6 N/m, and is the sum of the values shown in Tab. 2. With this value of the equivalent stiffness coefficient of the thrust bearing, the natural frequency of the system was estimated for a lumped parameters model (the single-degree-of-freedom equation, given by Eq. 1), by a finite element model (using linear and quadratic elements) and by the equation of longitudinal vibration of bars (known as the equation for continuous systems or the distributed parameters models, following the work of Peixoto, Vieira and Cavalca, 2015). These values are shown in Tab. 3. Since the distributed parameters is the actual governing equation for axial vibration of the turbocharger, this value is considered the reference in calculating the percentage difference between the approximated models.

Table 3 – Estimated first natural frequency of axial vibration of the turbocharger, for a rotation speed of 14,100 rpm

Model	ω_n (rad/s)	Percentage difference
Distributed parameters	6,375	-
Lumped parameters	6,383	0.133%
Linear finite element	6,684	4.85%
Quadratic finite element	6,707	5.22%

It can be argued from Tab. 3 that the lumped parameters model is good enough to observe the axial vibration of the turbocharger, since the natural frequency is almost the same for every model. The linear differential equation to model the one degree of freedom requires less computational effort of the solver in order to find the optimum value of the damping coefficient and is used instead of an analytical partial differential equation or a system of linear differential equations.

The value of the stiffness coefficient can also be checked calculating the new static equilibrium position under a step excitation with the same magnitude of the resultant of the forces shown in Tab. 2 acting on the system (Peixoto, 2016). The estimated oil film thickness was 24.2 μm, while the measured minimum oil thickness is 23.8 μm, which confirms the estimation of the equivalent stiffness coefficient. This value is adequate while running the optimization problem.

It is important to notice that the estimated stiffness coefficient is constant for the rotation speed of 14,100 rpm. This

coefficient is estimated based on the static equilibrium position of the system, for each rotational speed, after the system reaches steady state. The minor fluctuations in the rotational speed, typical of a turbocharger, does not alter the estimated stiffness coefficient. Vieira (2014) checked the variation of this coefficient with the rotational speed and the minor fluctuations in the speed are not enough to observe a difference on the estimated stiffness coefficient. Also, since the stiffness coefficient is estimated from the static equilibrium position, this parameter can be estimated disregarding the dynamic characteristics of the system, which is also the reason for not taken it into account on the optimization process. The only optimization variable is the damping coefficient. The damping coefficient is fundamentally a dynamic quantity, therefore the optimization problem takes into account the dynamic response of the system and the already estimated stiffness coefficient to estimate the damping coefficient.

The estimated damping coefficient is obtained solving the generalized Reynolds' Equation, now considering the $\partial h / \partial t$ term, applying a perturbation of velocity $\dot{h}$, giving a value of 6.165×10^3 N.s/m (Daniel, Vieira and Cavalca, 2016). Because of the lack of information on the variables that influence the estimation of the damping coefficient, this estimated value for the equivalent damping coefficient of the thrust bearings is not correct. This can be observed when integrating the equation of motion of the system (Eqs. 1-3), with the values obtained for the mass and the equivalent stiffness and damping coefficients, as shown in Fig. 6. Consequently, it is necessary to find the correct equivalent damping factor, which is done by optimizing this parameter, so the simulated response gets closer to the experimental results.

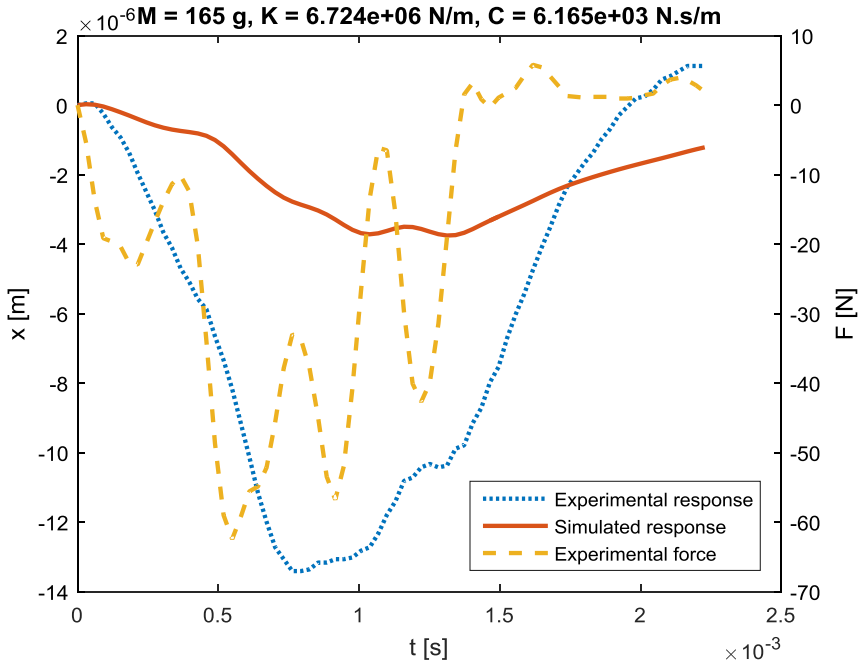

Figure 6 – Comparison between simulated and experimental results (with original estimation of equivalent damping coefficient)

Setting Eqs. 1-3 as the equations of motion of the system and with the value of the total mass of the system and the stiffness coefficient, the damping coefficient can be estimated by the optimization problem defined by Eq. 7. It must be observed that the damping coefficient was optimized during the transient response of the system, which limits the time duration of the impulse applied by the hammer (Fig. 7a) and the observed axial displacement (Fig. 7b). It must be also noted that, due to fluctuations in the measured force, the damping coefficient identification was carried on under two conditions of external forces: 1 – considering the experimental measurements of the external force (dotted blue line); 2 – considering the adjusted force, without considering these fluctuations (solid red line), as shown in Fig. 7a. The solid curve is the force utilized in the optimization algorithm, while the dotted line is the force measured in the impact hammer, during the time considered.

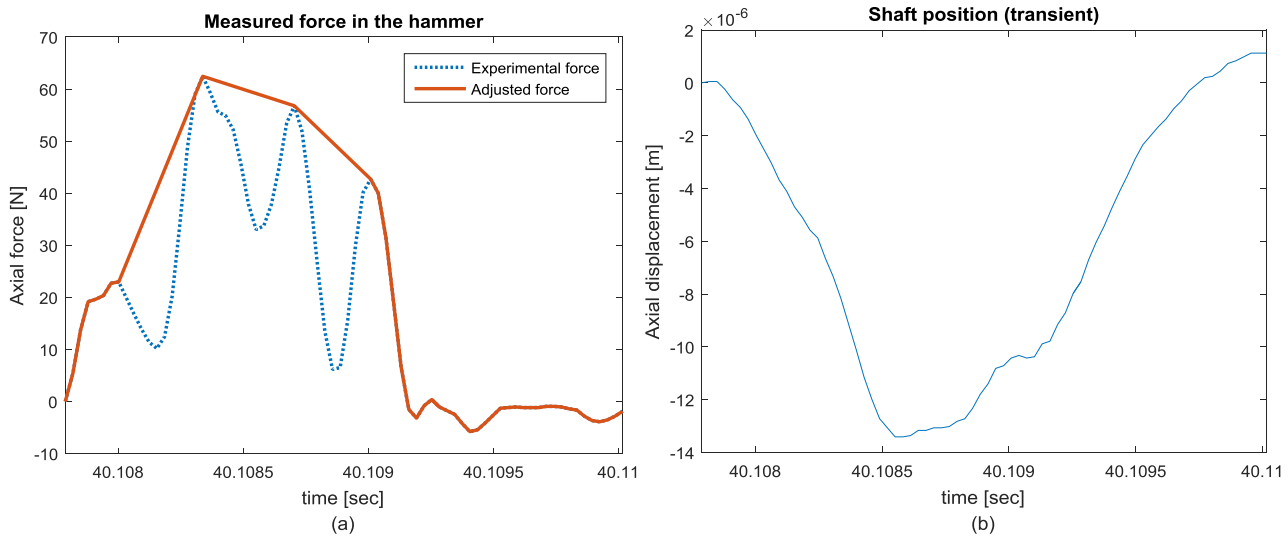

Figure 7 – Parameters considered during the optimization problem: (a) Adjusted experimental force and (b) Transient shaft displacement during the force application

The displacement of the shaft considered in the optimization is shown in Fig. 7b. It covers the same amount of time of the force and is only the transient response of the shaft. This is the experimental displacement considered to optimize the damping coefficient of the system.

Utilizing the value of 6.724×10^{6} N/m for the stiffness coefficient, the experimental force shown in Fig. 7a (dotted line), the shaft displacement of Fig. 7b and the total mass of 165 g, the first optimization of the damping coefficient returns a value of 1.090×10^{3} N.s/m. The dynamic response of the system to the external excitation given by an impact hammer is shown in Fig. 8. The optimization problem was run with a small tolerance for the objective function, to ensure the value obtained is the global minimum, not a local minimum. The initial value used for the algorithm was the previously calculated damping coefficient of 6.165×10^{3} N.s/m.

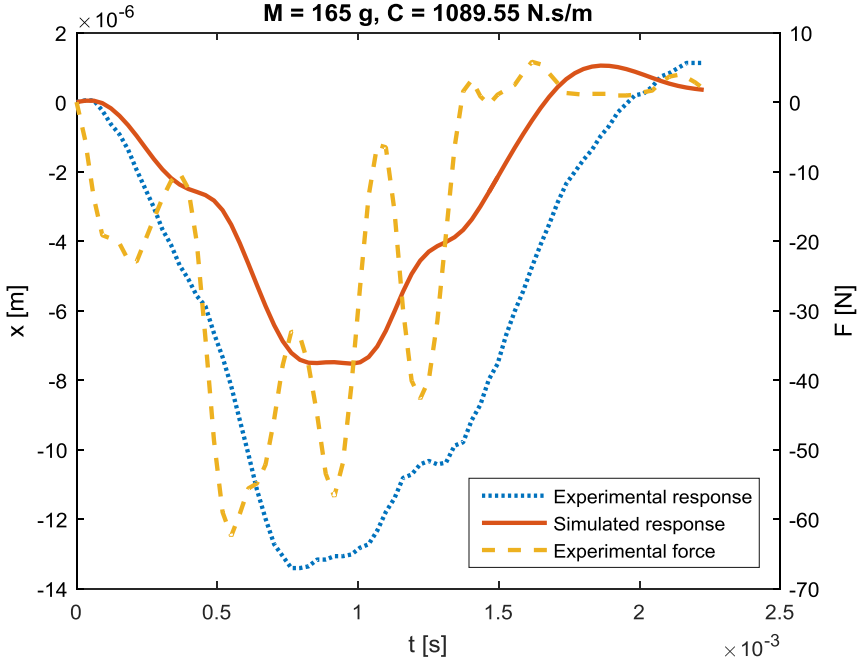

Figure 8 – Comparison between simulated and experimental results (optimization run with experimental force)

It can be seen from Fig. 8 that the general behavior tendency of the displacement of the shaft given by the simulations is the same as the experimental results. However, the amplitude of the displacement is not still in good accordance between both curves. A second optimization was carried on, using the adjusted force shown in Fig. 7a (solid line), not accounting for the minor fluctuations in the experimental measured forces. This optimization returns a value for the damping coefficient of 1.121×10^{3} N.s/m and the dynamic response for this system is shown in Fig. 9, bringing a better accordance between the experimental and simulated displacement of the collar clamped to the shaft.

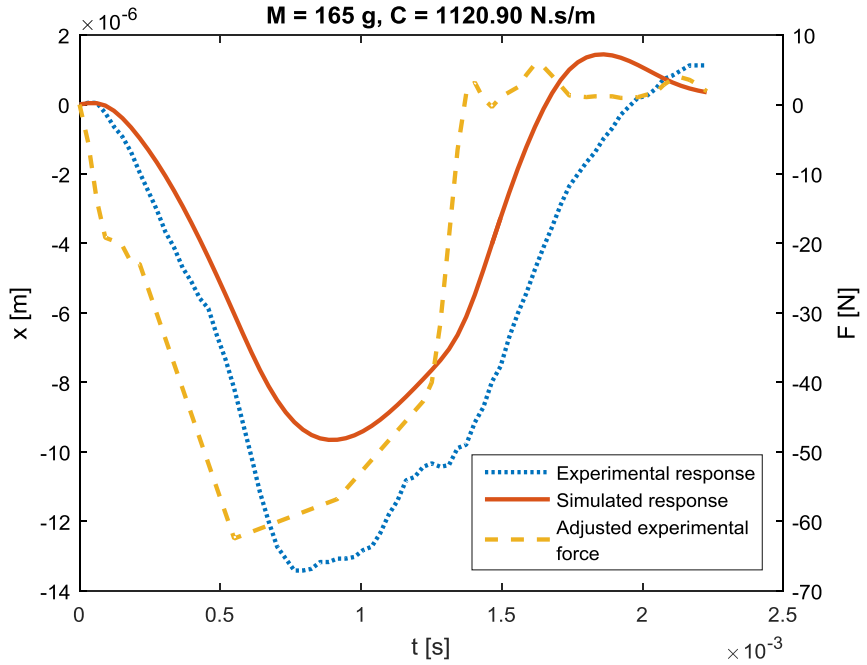

Figure 9 – Comparison between simulated and experimental results (optimization run with adjusted force)

Using the value of the initial estimated equivalent damping coefficient, the damping factor ξ of the system is estimated in 2.92, whereas the damping factor utilizing the value for the damping coefficient obtained from the second optimization (Fig. 9) is 0.532. From the agreement between the curves of Fig. 9 and the more plausible value for the damping factor, it can be said that the original value estimated for the damping coefficient was not adequate. One can assume that, for this particular system, the perturbation model utilized to approach the damping factor may be not well suited. Moreover, in turbochargers, one aim is to reduce vibrations to a minimum. For a desirable transient response, the damping factor must be between 0.4 and 0.8, which was satisfactorily obtained, because small values of ξ (that is, $\xi < 0.4$) yield excessive overshoot in the transient response, and a system with a large value of ξ (that is, $\xi > 0.8$) responds sluggishly (Ogata, 2010). This is achieved by designing a thrust bearing with a relative high damping factor. However, overdamped systems, although do not present vibrations, respond slower, i.e., the settling time is usually higher than the settling time of systems with a damping ratio close to unity. Therefore, the value of 0.532 for this system is more acceptable and suitable for the thrust bearing performance.

Finally, it is also important to notice that the adjusted experimental force utilized on the simulations seems more appropriate. The spikes observed on the measured experimental force (Fig. 7a) are probably due to sensors limitations (measurements time of nearly 1ms), since the experimental response of the system does not have spikes accompanying the input force. Moreover, the simulations disconsidering the spikes on the input force provide a better response, which is another indication that the correct force applied by the hammer is just one single impact on the turbocharger.

CONCLUSIONS

With the damping coefficient obtained from the second optimization, the damping factor is 0.532, which indicates that this system is underdamped and its impulse response decays fast enough. The difference in amplitude of the measured displacement and the simulated response with the adjusted force is about 4 μm. Besides, the oscillation frequency of the simulated response approaches the frequency of the experimental results, as observed in Figs. 7b and 9, because both curves have the same shape.

It must also be noted that the numerical integration of the system must be made utilizing the experimental force as an input. Although the force applied by the impact hammer approaches an impulsive excitation, which could be modeled using the Dirac delta function, the fundamental period of the system (the inverse of the natural frequency) is about 1×10^{-3} s, so the input of the system cannot be approximated by an impulse. This approximation is only valid if the time duration of the force is much smaller than the fundamental period of the system, which is not true for the case in analysis.

Furthermore, two other important points must be noted. First, because of the high rotational speed of the system, the estimation of the stiffness coefficient must be made utilizing a thermo-hydrodynamic model, because there is heat generated by viscous dissipation, due to fluid shear. This must be taken into account, even for steady state operation, which gives a good estimate for the stiffness coefficient. To do a THD analysis on the thrust bearing, the inlet temperature of the oil must be known. This temperature was estimated utilizing a THD model to obtain the outlet temperature of the oil leaving the journal bearings of the turbocharger. Once the stiffness coefficient is obtained, the damping coefficient can be estimated.

The second important point here is that the damping coefficient is estimated by an optimization problem, requiring that the dynamic response of the system must be close enough to experimental measured results. These estimated coefficients are nearly constant for the rotational speed of the system, since minor variations on the rotational speed provokes little variation on these coefficients. The order of magnitude of these variations are much smaller than the order of magnitude of these parameters, so the estimates are promising to simulate dynamic response of systems in steady state conditions.

ACKNOWLEDGMENTS

The authors would like to thank the BorgWarner, Inc company and the Student Support Service at Unicamp (SAE) for the financial support of this project.

REFERENCES

Ahmed, S. A., Fillon, M., Maspeyrot, P., 2010, Influence of Pad and Runner Mechanical Deformations on the Performance of a Hydrodynamic Fixed Geometry Thrust Bearing, Proc. of the Institution of Mechanical Engineers, v. 224, part J: Journal of Engineering Tribology, pp. 305-315.

Almqvist, T., Glavatskih, S. B., Larsson, R., 2000, THD Analysis of Tilting Pad Thrust Bearings – Comparison Between Theory and Experiments. Transactions of the ASME, v. 122, pp. 122-417.

Arghir, M.; Alsayed, A.; Nicolas, D., 2002, The Finite Volume Solution of the Reynolds Equation of Lubrication with Film Discontinuities, International Journal of Mechanical Sciences, v. 44.

Byrd, R. H., Gilbert, J. C., Nocedal, J., 2000, A Trust Region Method Based on Interior Point Techniques for Nonlinear Programming, Mathematical Programming, v. 89, No. 1, pp. 149–185.

Byrd, R. H., Hribar, M. E., and Nocedal, J., 1999, An Interior Point Algorithm for Large-Scale Nonlinear Programming, SIAM Journal on Optimization, v. 9, No. 4, pp. 877–900.

Dadouche, A., Fillon, M., Bligoud, J. C., 2000, Experiments on Thermal Effects in a Hydrodynamic Thrust Bearing, Tribology International, v. 33, pp. 167-174.

Dadouche, A., Fillon, M., Dmochowski, W., 2006, Performance of a Hydrodynamic Fixed Geometry Thrust Bearing: Comparison between Experimental Data and Numerical Results, Tribology Transactions, v. 49, pp. 419-426.

Daniel, G. B., Vieira, L. C., Cavalca, K. L, 2016, Sensitivity analysis of the dynamic characteristics of thrust bearings, 3rd International Symposium on Uncertainty Quantification and Stochastic Modeling, Vol. 1, Uberlândia, Minas Gerais, Brazil, pp. 1-10

Dowson, D. A., 1962, A Generalized Reynolds Equation for Fluid Film Lubrication, International Journal of Mechanical Sciences, 4, pp. 159-170

Hamrock, B. J., Schmid, S. R., Jacobson, B. O., 1994, Fundamentals of Fluid Film Lubrication. 2nd Ed, Ed.McGraw-Hill, New York, United States of America, 782 p.

Korpela, S. A., 2011, Principles of turbomachinery, Ed. John Wiley & Sons, New Jersey, United States of America, 480 p.

Lund, J. W., 1987, Review of the Concept of Dynamic Coefficients for Fluid Film Journal Bearings, ASME Journal of Tribology, 109, pp 37-41.

Müller, P. C., Schiehlen, W. O., 1985, Linear Vibrations – A theoretical treatment of multi-degree-of-freedom vibrating systems, Ed. Martinus Nijhoff Publishers, translated by Swierczkowski, S., Dordrecht, The Netherlands, 327 p.

Peixoto, T. F., Vieira, L. C., Cavalca, K. L, 2015, Analysis of rotors supported by thrust bearings, 23rd ABCM International Congress of Mechanical Engineering, Rio de Janeiro, Brazil, pp. 1-8

Peixoto, T. F., 2016, Analysis of rotors supported by thrust bearings, Master's thesis, University of Campinas, Faculty of Mechanical Engineering, retrieved from <http://www.bibliotecadigital.unicamp.br/document/?code=000972180>

Pinkus, O., Lynn, W., 1958, Solution of the Tapered-Land Sector Thrust Bearing, Transactions of ASME, v. 80, pp. 1510-1516.

Ogata, K., 2010, Modern Control Engineering, 5th Ed., Ed. Prentice Hall, Upper Saddle River, New Jersey, United States of America, 905 p.

Reynolds, O., 1886, On the Theory of Lubrication and its Application to Mr. Beauchamp Tower's Experiments, including an Experimental Determination of the Viscosity of Olive Oil. Philosophical Transactions of Royal Society of London, 177, Part 1, n. Series A, pp. 157-234.

Vieira, L. C., 2014, Analysis of a thermohydrodynamic model for thrust bearings, Doctoral dissertation, University of Campinas, Faculty of Mechanical Engineering, retrieved from <http://www.bibliotecadigital.unicamp.br/document/?code=000943088>

RESPONSIBILITY NOTICE

The authors are the only responsible for the material included in this paper.